

SUPPORTING INFORMATION:

**Reducing Dilution and Analysis Time in Online Comprehensive Two Dimensional  
Liquid Chromatography using Active Modulation**

Andrea F.G. Gargano<sup>1,2</sup>, Mike Duffin<sup>3</sup>, Pablo Navarro<sup>3</sup>, Peter J. Schoenmakers<sup>2</sup>

<sup>1</sup> *TI-COAST, Van 't Hoff Institute for Molecular Sciences, Science Park 904, 1098 XH Amsterdam, Netherlands*

<sup>2</sup> *Van 't Hoff Institute for Molecular Sciences, Science Park 904 1098 XH Amsterdam, Netherlands*

<sup>3</sup> *Syngenta, Jealott's Hill International Research Centre, Bracknell, Berkshire RG42 6EY, UK*

(\*) corresponding author

E-mail: a.gargano@uva.nl

## TOC of the supporting information

<b>S1.</b>	<b>Comparison of the TSPs separation using different HILIC stationary phases .....</b>	<b>3</b>
<b>S2.</b>	<b>LC-MS analysis of TSPs .....</b>	<b>4</b>
<b>S3.</b>	<b>Assignment of LC×LC peaks .....</b>	<b>14</b>
<b>S4.</b>	<b>Effect of injection volume on the separation efficiency .....</b>	<b>15</b>
<b>S5.</b>	<b><sup>2</sup>D Gradient with different <math>t_G/t_0</math> .....</b>	<b>16</b>

## S1. Comparison of the TSPs separation using different HILIC stationary phases

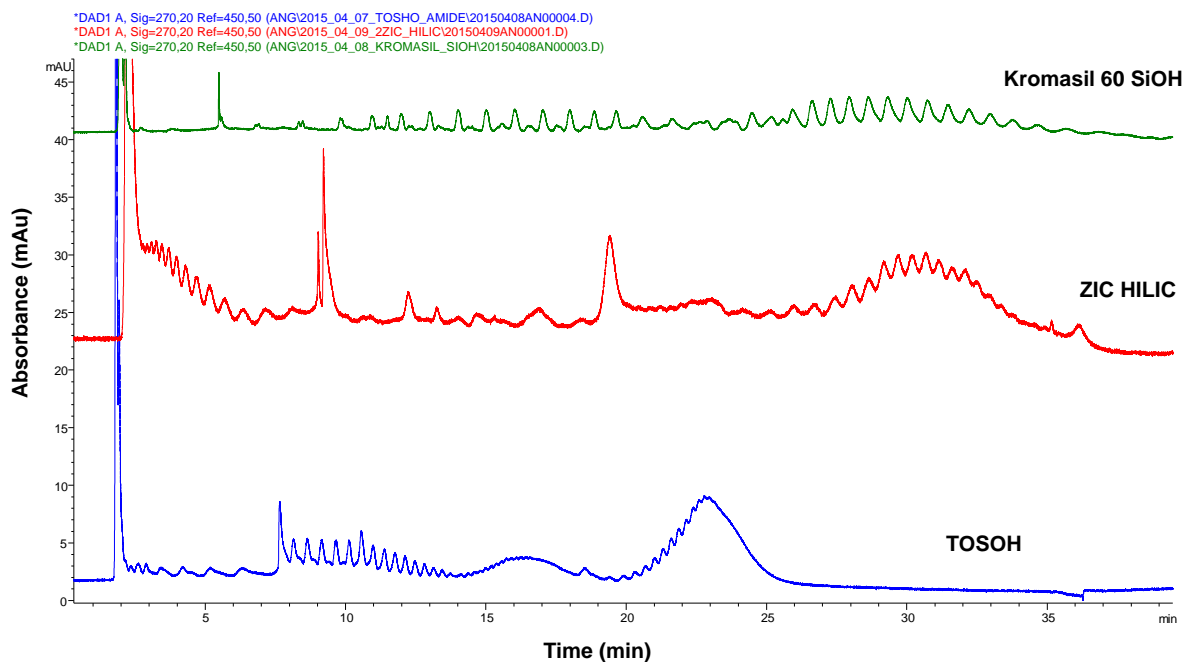


**Figure S1:** Overlay of the chromatograms obtained by the injection of A16A (1 mg/mL in ACN; 5  $\mu$ L injection) using Kromasil SiOH, ZIC HILIC, TOSOH columns. Conditions: MPA=ACN, MPB= 25 mM CH<sub>3</sub>CHOONH<sub>4</sub>. Columns tested: Kromasil SiOH\* (3.2 x 250 mm 5  $\mu$ m), Sequant ZIC HILIC (two of 150 of 2.1 x 150 mm 5 $\mu$ m), TOSOH Amide (2.1 x 250 mm 5 $\mu$ m).

Flow rate: 0.35mL/ min; T= 15 C (\*0.81 mL/ min, flow rate increased in order to have comparable linear flow velocity). Linear Gradient 0to 30% B in 30 min, 5 min 30%B, 15 min riequilibrium

## S2. LC-MS analysis of TSPs

The analysis of the TSP samples was carried out using a UPLC system (Waters UPLC Acquity) coupled to a triple quadrupole mass spectrometer (ThermoFisher Discovery). The scanning range was set to 50 to 1500 m/z, 0.7 units and the acquisition time was of 0.5 s per each scan (2 Hz). A splitter was used to control the flow rate going to the ESI interface and the split was changed depending on the chromatographic flow rate adopted in order to have approximately 300  $\mu\text{L}/\text{min}$  of flow rate to the source. Samples were prepared as 1 mg/ mL solution and the injection volume was set to 10  $\mu\text{L}$ . For the RP separation we used a Phenomenex Kinetex C-18 (4.6 x 50 mm, 2.6  $\mu\text{m}$  particles) and the NP separation was carried out with a Waters Acquity UPLC BEH HILIC column (2.1x 150 mm, 130A, 1.7  $\mu\text{m}$ ).

## RP Characterization

The gradient was set at 5 min with a flow rate of 1 mL/min (total analysis time 8 min; details reported in figure S1).

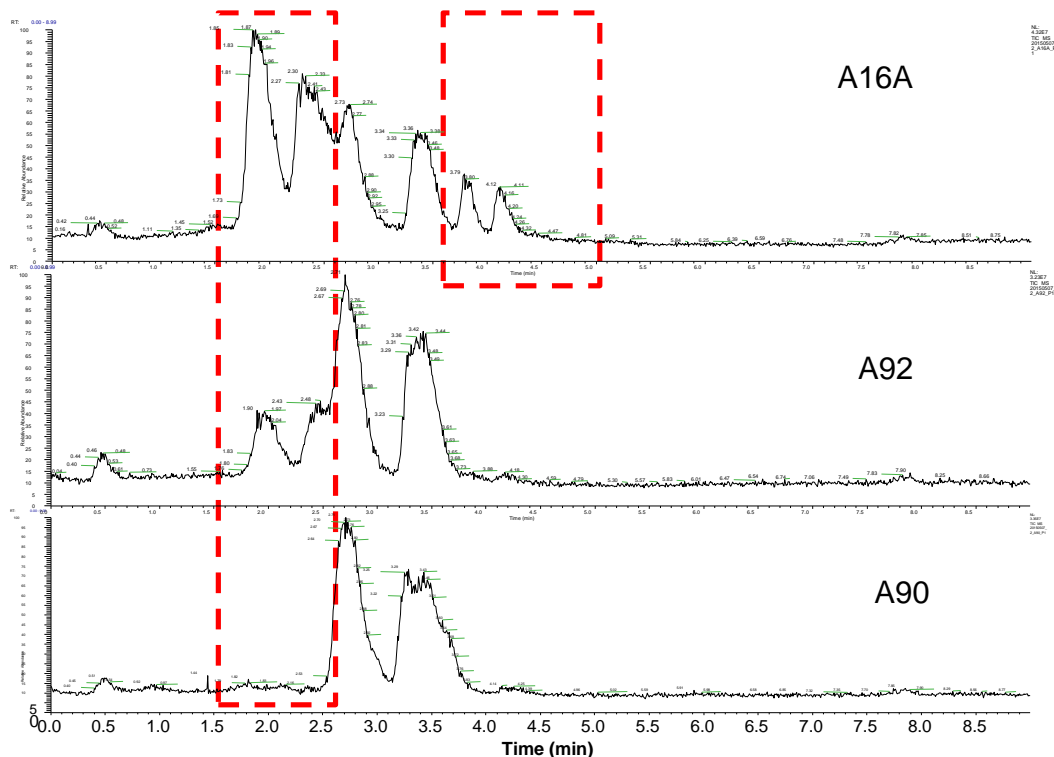


**Figure S2:** Total Ion Current Chromatogram of samples A16A (Agnique PE TSP 16A) A92 (Agent 3152-92) and A90 (Agent 3152-90). In the red boxes are marked the differences between the different analytes. Conditions: Flow rate= 1 mL/min, MPA=25mM Ammonium Acetate + 1% 1-BuOH, MPB= MeOH + 1% BuOH. Linear Gradient 50 to 100% B in 5 min.

On the basis of the MS data we identified anionic (phosphated) and non-ionic Di and Tri Styryl Phenyl Ethoxylates. The fast gradient conditions allowed the separation of the polymeric species under (pseudo) critical conditions, hence the components were separated on the basis of their chemical composition, independently of their molecular weight (determined by the number of ethoxy units).

In the following pages are shown the results from A16A (Agnique PSE 16A), this compound has non-ionic, anionic fractions as well as an additional impurity and thus presents the higher number of species in the analysis sample set.

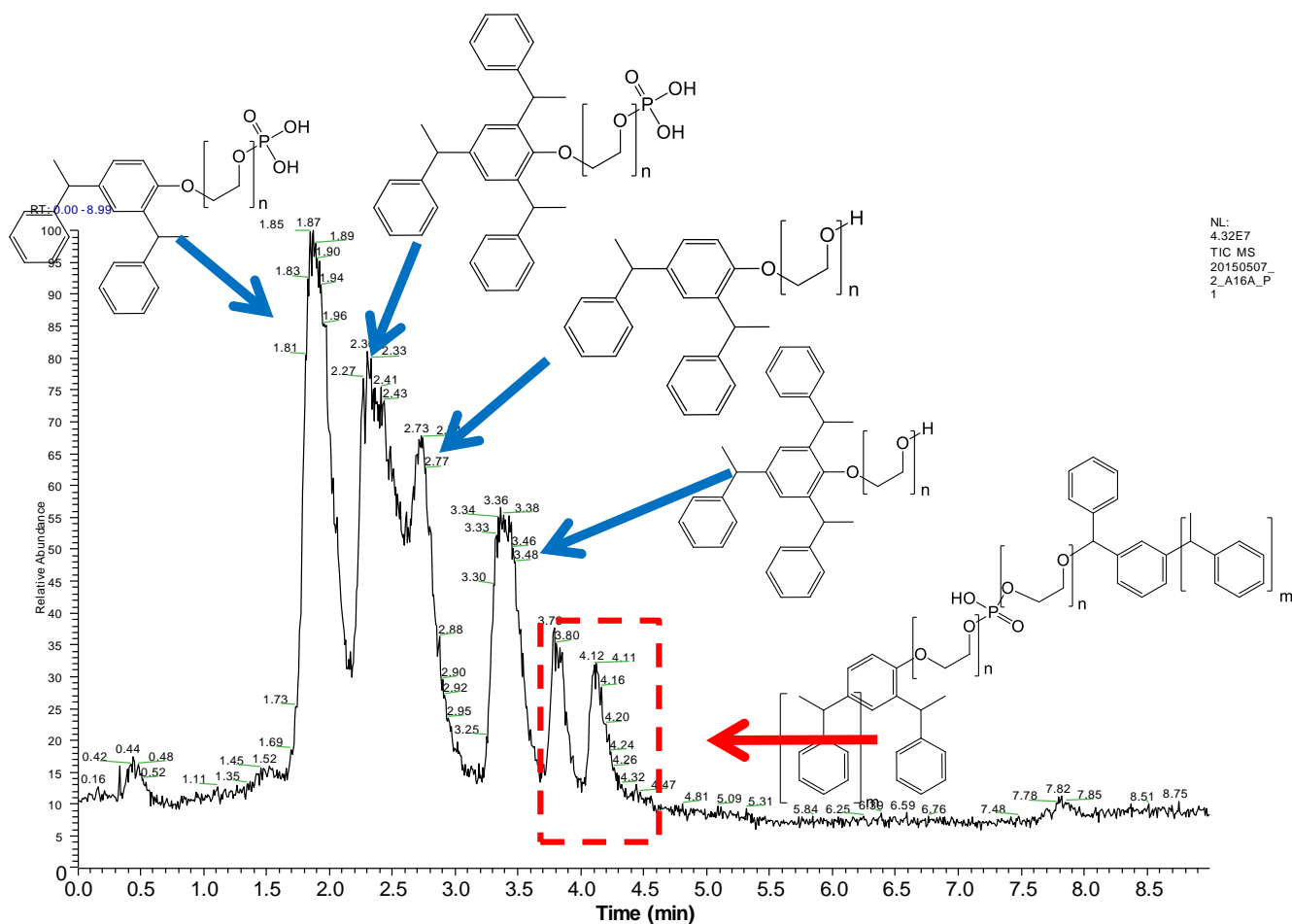
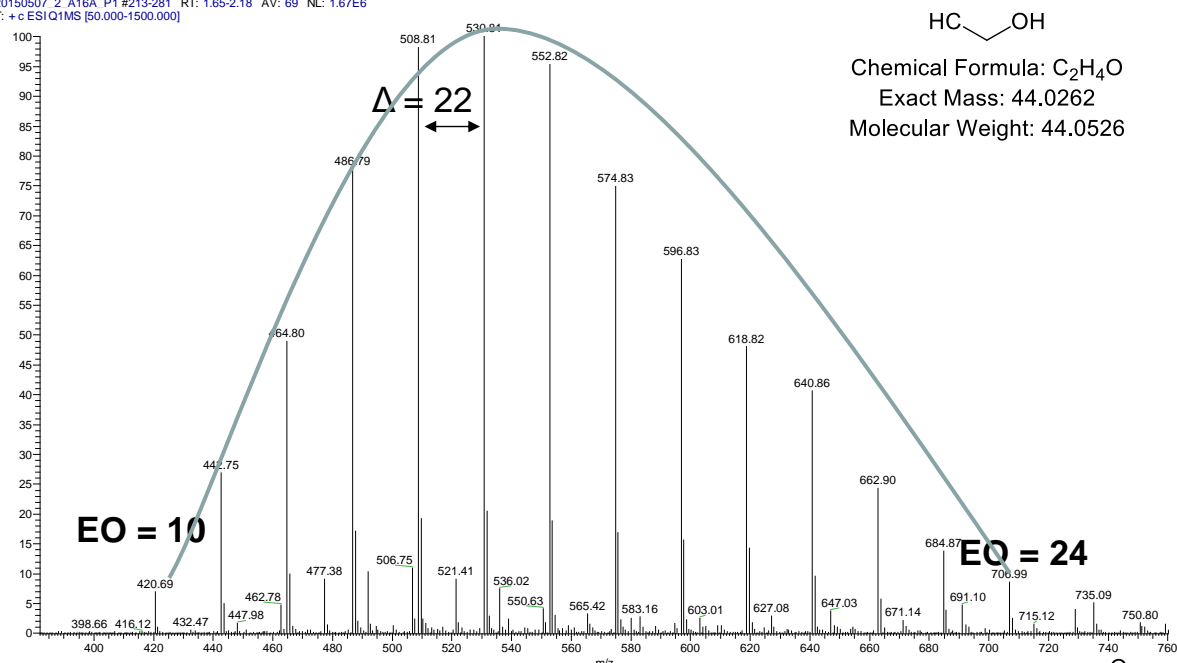


**Figure S3:** Identification of the peaks from the Reversed Phase analysis of surfactant Agnique PSE 16A. The red box indicates the structure of the additional impurity of this surfactant. Details about the peak assignment are reported in the next figures. The chromatographic parameters are reported in figure S2.

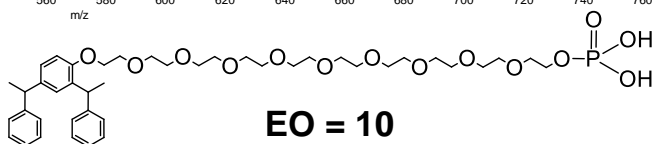
Figure S4 shows the  $m/z$  of for the first eluting peak in Figure S3. This peak corresponded to the elution of distyryl phenoxy ethoxylate phosphate. Species with an ethoxylation number varying from 10 to 24 were identified. Similarly, in Figure S 4, 5, 6 we identified the tri styryl phenoxy ethoxylate phosphate, di styryl phenoxy ethoxylate and tri styryl phenoxy ethoxylate. The additional peaks eluting at the end of the chromatogram were tentatively identified as by-products generated by the additional reaction of the di (or tri) styryl phenoxy ethoxylate phosphate units with ethoxylate with the di (or tri) styryl phenoxy ethoxylate compounds. Their mass spectra are reported in figure S7 and S8.

20150507\_2\_A16A\_P1\_#213-281 RT: 1.65-2.18 AV: 69 NL: 1.67E6  
T: +c ESI Q1 MS [50.000-1500.000]



$z = 2; [M + H + NH_4]^{2+}$

$m = (420.69 \times 2) - (18+1) = 822.38$



Chemical Formula:  $C_{42}H_{63}O_{14}P$

Exact Mass: 822.40

Molecular Weight: 822.91

**Figure S4:** Full ion scan mass spectrometry scan of the first eluting peak of the reversed phase separation reported in Figure S3. The mass spectrometry conditions and chromatographic conditions are reported in the LC-MS introduction chapter.

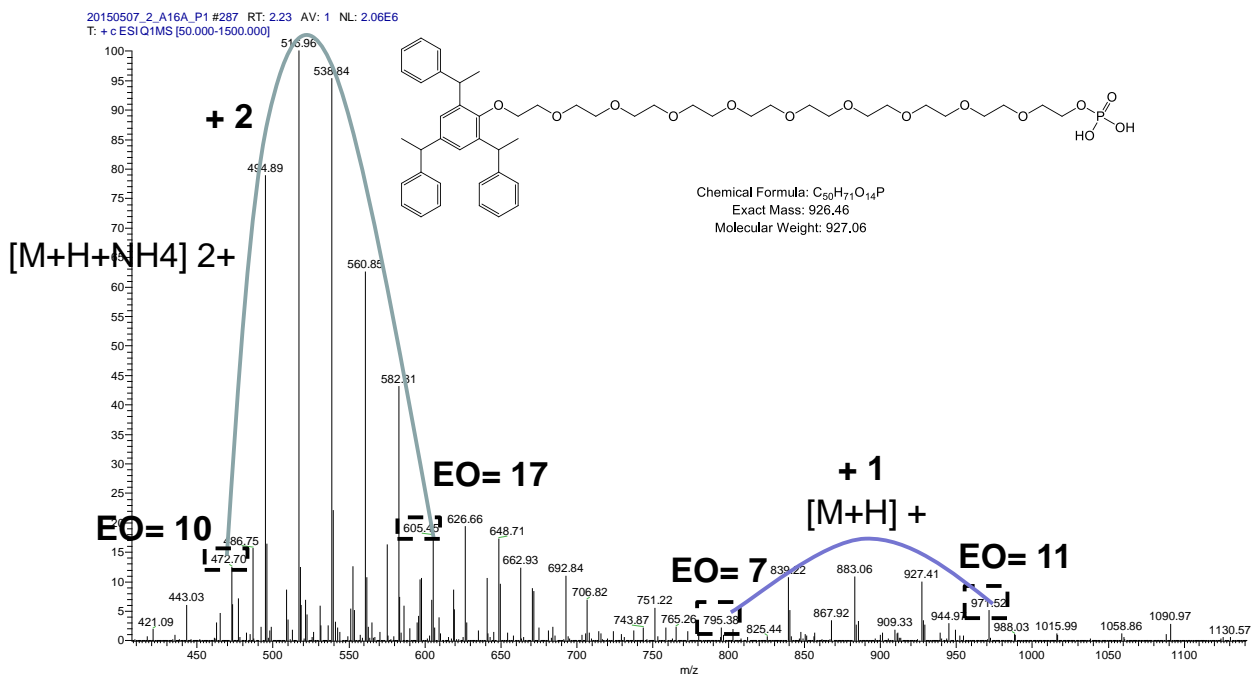


**Figure S5:** Full ion scan mass spectrometry scan of the second eluting peak of the reversed phase separation reported in Figure S3. In the figure are identified both the single and doubly charged species. The mass spectrometry conditions and chromatographic conditions are reported in the LC-MS introduction chapter.



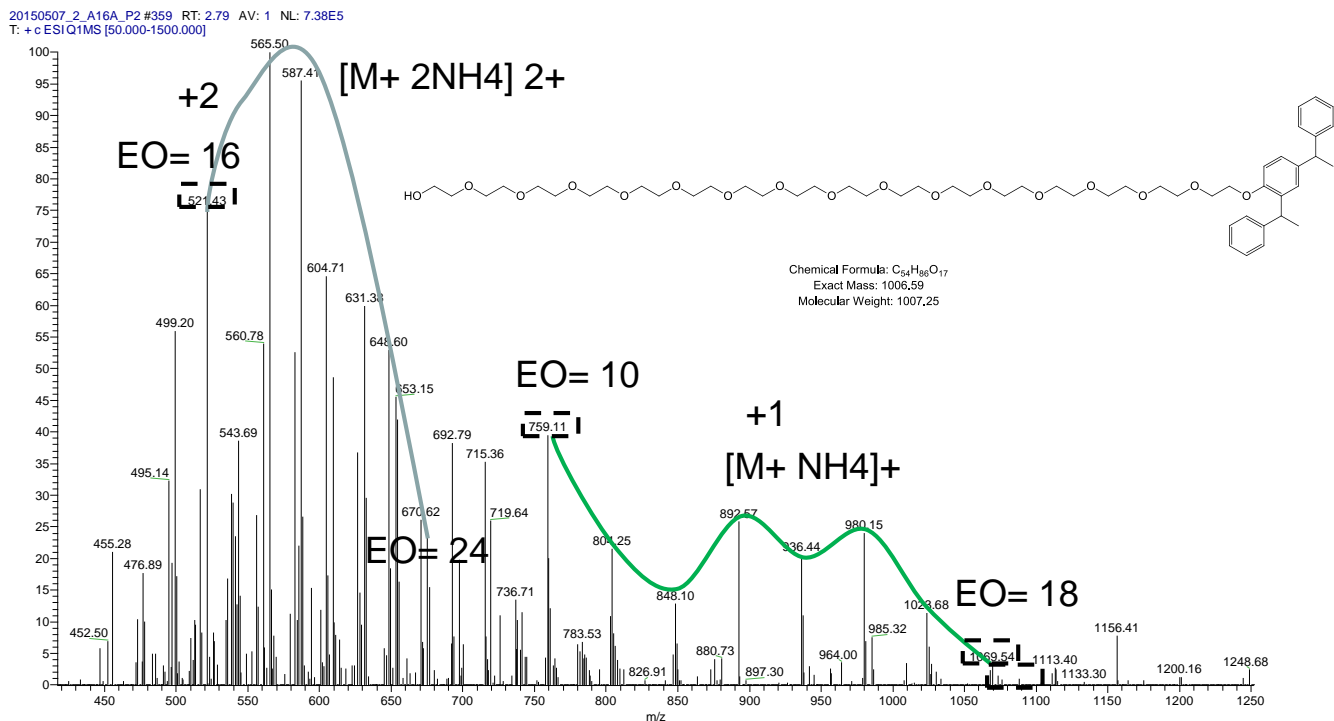


**Figure S6:** Full ion scan mass spectrometry scan of the third eluting peak of the reversed phase separation reported in Figure S3. In the figure both the single and doubly charged species are identified. The mass spectrometry conditions and chromatographic conditions are reported in the LC-MS introduction chapter.

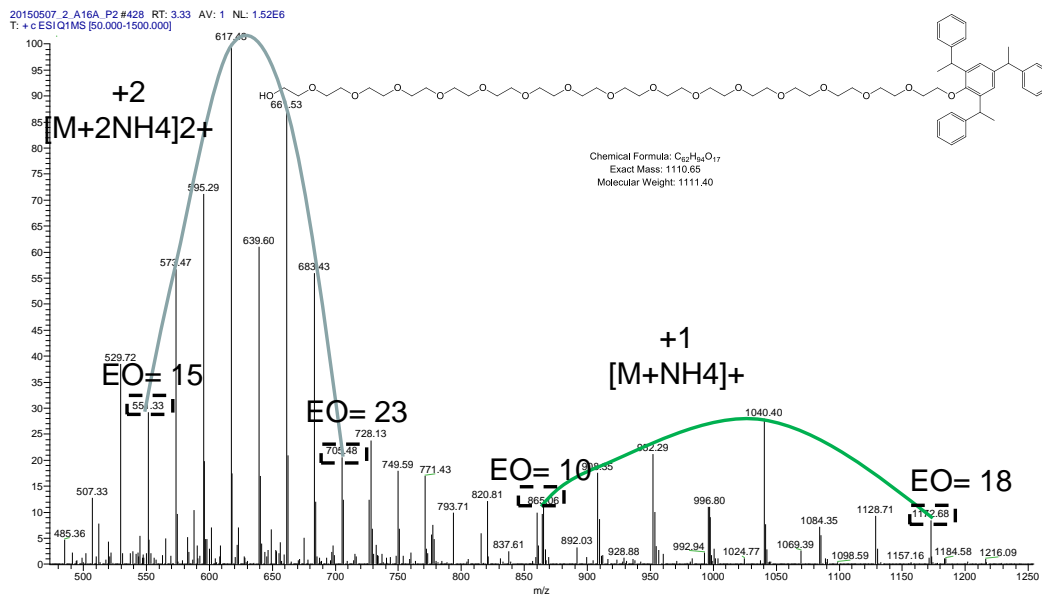


**Figure S7:** Full ion scan mass spectrometry scan of the fourth eluting peak of the reversed phase separation reported in Figure S3. In the figure are identified both the single and doubly

charged species. The mass spectrometry conditions and chromatographic conditions are reported in the LC-MS introduction chapter.

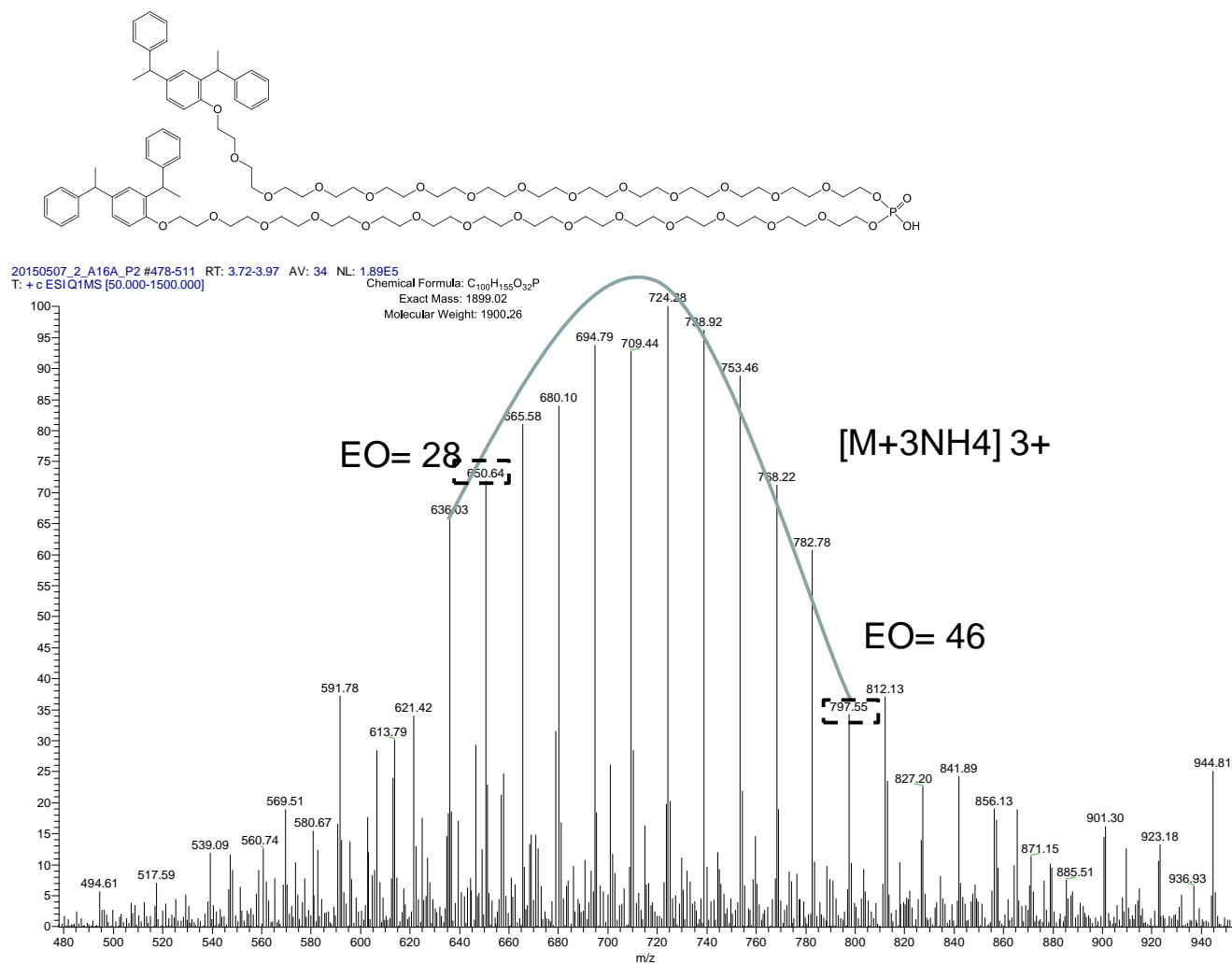


**Figure S8:** Full ion scan mass spectrometry scan of the fifth eluting peak of the reversed phase separation reported in Figure S3. The mass spectrometry conditions and chromatographic conditions are reported in the LC-MS introduction chapter. The figure illustrate the tentative structure of the compound identified according to the MS spectra

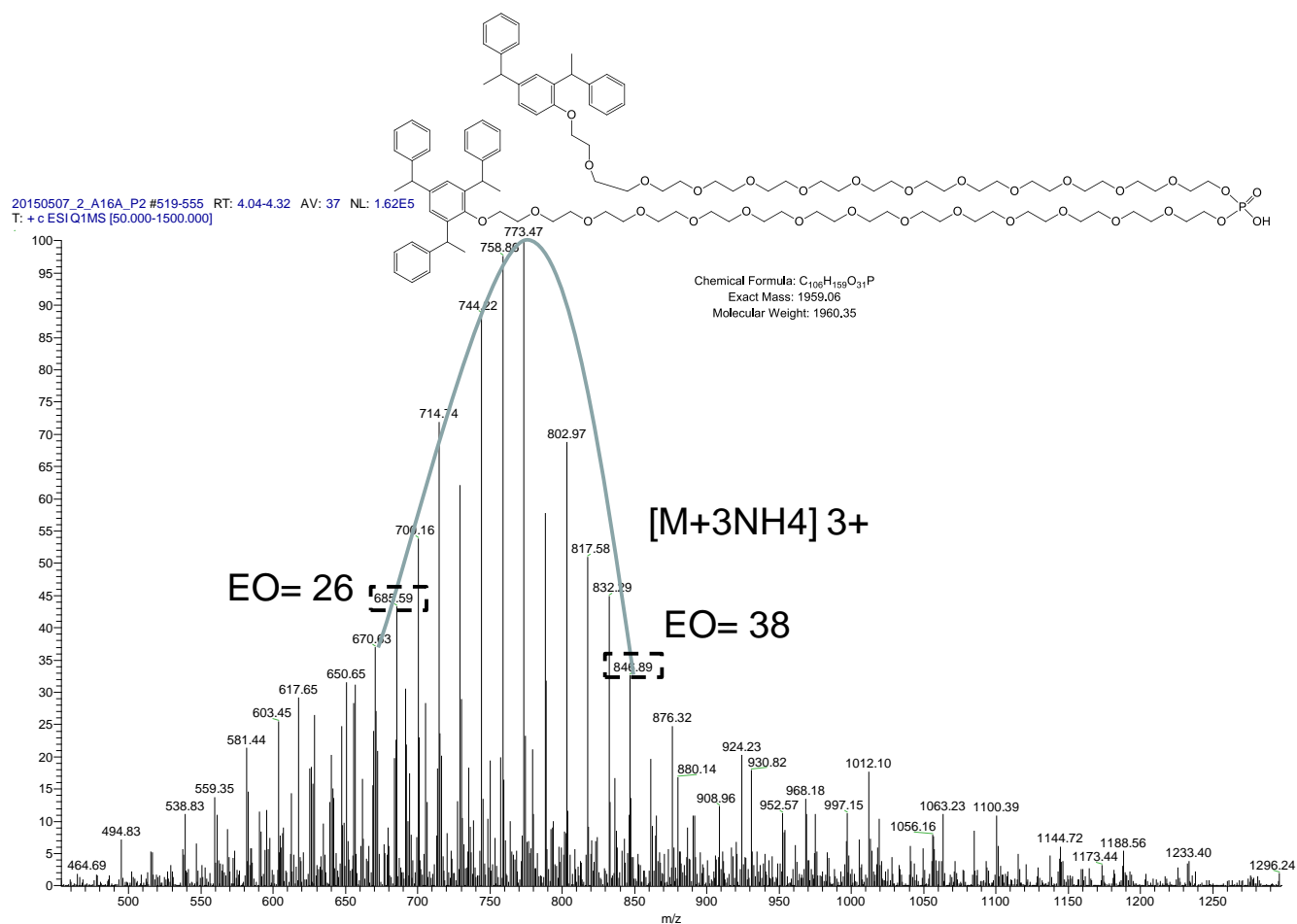


**Figure S9:** Full ion scan mass spectrometry scan of the sixth eluting peak of the reversed phase separation reported in Figure S3. The mass spectrometry conditions and chromatographic conditions are reported in the LC-MS introduction chapter. The figure illustrate the tentative structure of the compound identified according to the MS spectra

## HILIC Phase Analysis

In order to confirm the separation in the first dimension we studied the HILIC separation using the Waters Acquity BEH HILIC (2.1 x 150 mm with 1.7  $\mu\text{m}$  130 A particles) and a mobile phase gradient from 2 % 25mM ammonium acetate in 98% ACN to 50% 20mM ammonium acetate in ACN in 20 min. The results confirmed the separation of the TSPs on the basis of their number of ethoxylate units (from lower to higher number). Di and Tri Styryl Phenoxy Ethoxylate series were not separated chromatographically. As in the case of the RP separation here are collected the results obtained from Agnique PSE 16A since it's the compound that presents a higher level of heterogeneity (Figure S9).

The first eluting compounds are the di styryl followed by the tri styryl ethoxylates. Peaks from the two series of compounds are overlapping. Peaks assigned to the by-product originating from styryl ethoxylate and styryl ethoxilate phosphate units reacted together are eluting as a third compound group and the last area is represented by the phosphorylated compounds.

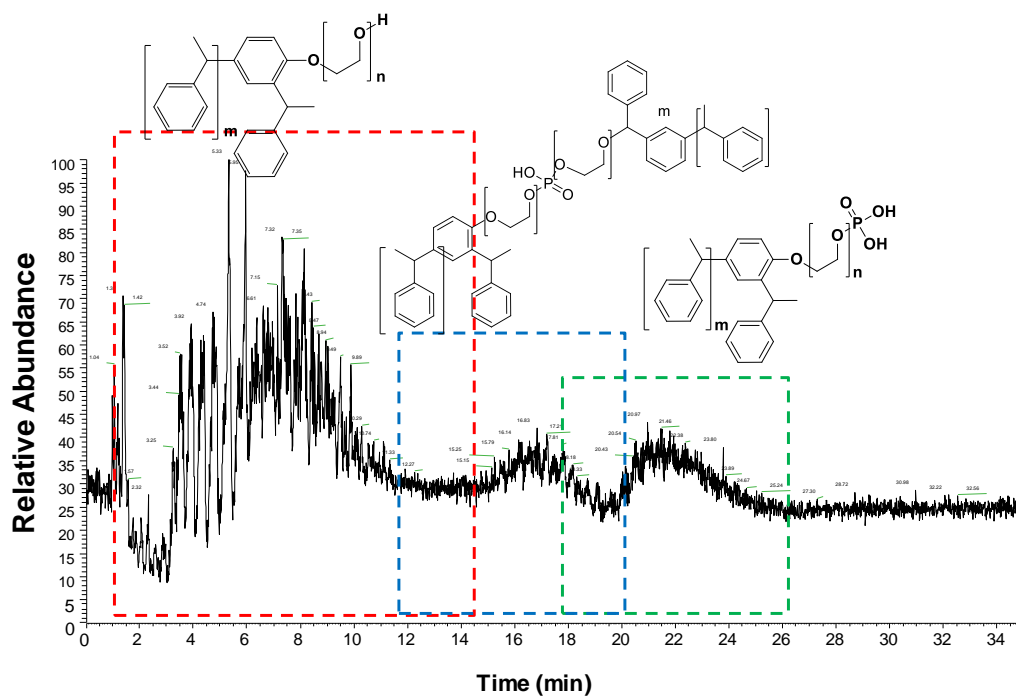


**Figure S10:** LC-MS chromatogram from the analysis of the surfactant A16A showing the species identified. The blue box indicates the structure of the additional impurity of this surfactant. Details about the peak assignment are reported in the next figures. Flow rate: 1 mL/ min. MPA: 98% ACN 2% 25 mM Ammonium Acetate, MPB: 25mM Ammonium Acetate. Linear gradient 0-50% B in 20 min.

In Figure S10 the mass spectra of the peaks from the first area of the separation shown in figure S9 are reported. The first eluting peaks are given by singly charged ammonium adduct of TSPs, separated on the basis of their degree of ethoxylation.

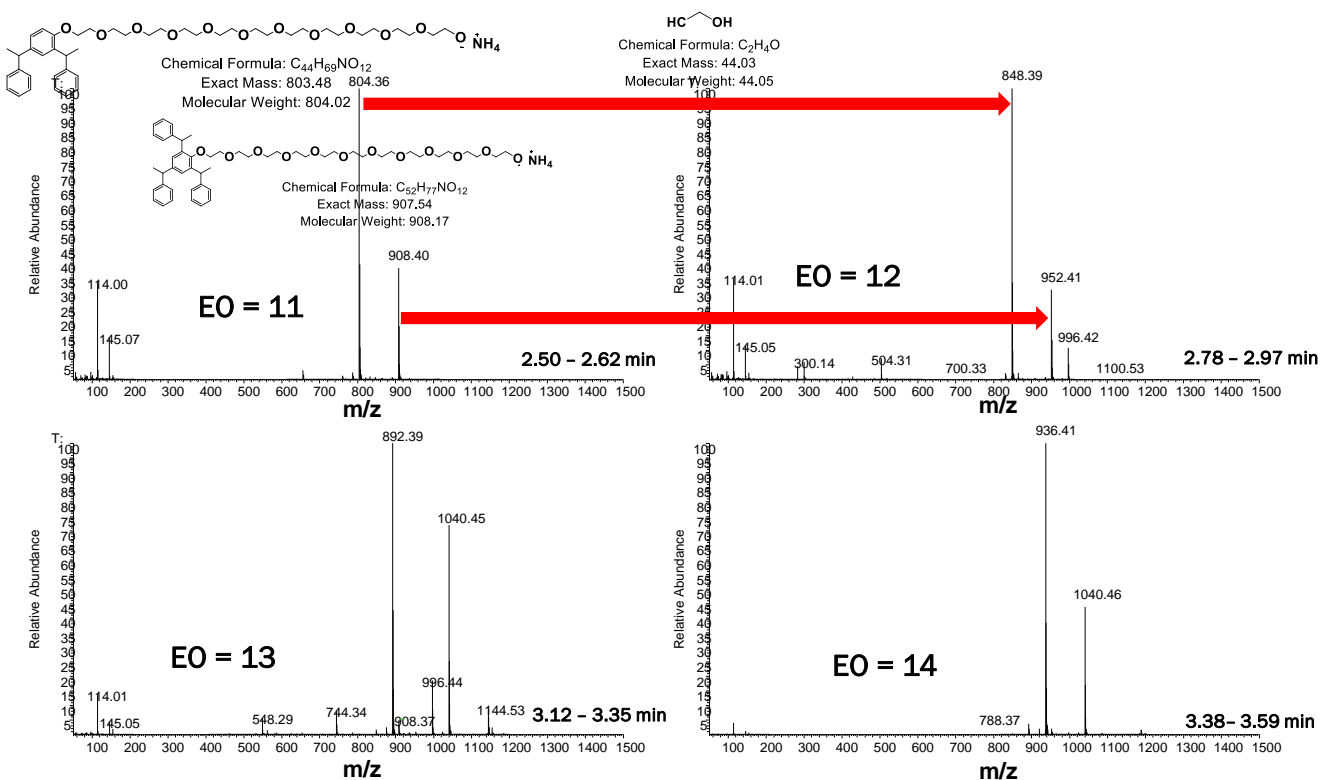


**Figure S11:** Mass spectrometry scans of the peaks eluting from 2.5 to 3.59 minutes in Figure S10, showing the separation of the different ethoxylates using normal phase separation conditions.

### S3. Assignment of LC×LC peaks

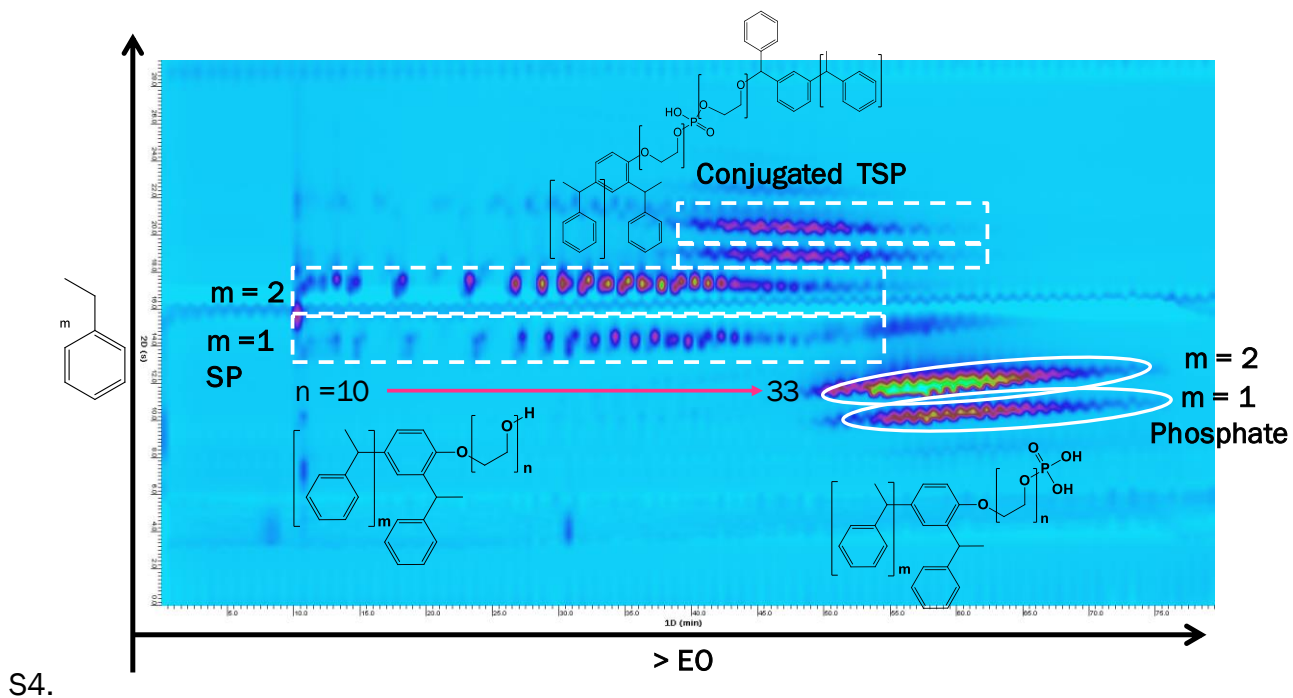


**Figure S12:** Two dimensional chromatogram of the analysis of Agnique TSP 16A showing the assigned peaks on the basis of the LC-MS results. Conditions:1D: Waters BEH HILIC (2.1 x 150 mm 1.7  $\mu\text{m}$ , 130  $\text{\AA}$ ). Conditions as reported in the instrumentation, conditions and data analysis section of the article.

### S5. Effect of injection volume on the separation efficiency

**Table S1:** Effect of the gradient time ( $t_g$ ) and of the injection volume on the peak capacity of the reverse phase separation of Agnique TSP 16A. Mobile phase conditions as in Figure 4 of the manuscript.

		<b>1 min (<math>t_g = 0.8</math>)</b>		<b>0.5 min (<math>t_g = 0.35</math>)</b>		<b>0.35 min (<math>t_g = 0.23</math>)</b>	
<b>V Inj</b>	<b>Peak</b>	<b>Time (min)</b>	<b>Width (1/2 h)</b>	<b>Time (min)</b>	<b>Width (1/2 h)</b>	<b>Time (min)</b>	<b>Width (1/2 h) (min)</b>
<b>20 <math>\mu</math>L</b>	1	0.36	0.028	0.3	0.016	0.28	0.015
	2	0.44	0.022	0.34	0.017	0.3	0.011
	3	0.48	0.025	0.39	0.018	0.33	0.023
	4	0.58	0.023	0.46	0.018	0.38	0.027
	5	0.65	0.017	0.5	0.014	0.45	0.02
	6	0.69	0.019	0.53	0.014	0.48	0.022
		Av.	0.022	<b>Av.</b>	<b>0.016</b>	Av.	0.02
		<b>n<sub>c</sub></b>	22.13	<b>n<sub>c</sub></b>	<b>13.79</b>	<b>n<sub>c</sub></b>	7.85

<b>V Inj</b>	<b>Peak</b>	<b>Time</b>	<b>Width</b>	<b>Time</b>	<b>Width</b>	<b>Time</b>	<b>Width</b>
<b>0.1 <math>\mu</math>L</b>	1	0.37	0.022	0.3	0.017	0.25	0.013
	2	0.44	0.021	0.36	0.017	0.29	0.014
	3	0.5	0.016	0.41	0.013	0.34	0.016
	4	0.59	0.02	0.47	0.017	0.41	0.015
	5	0.65	0.016	0.5	0.014	0.42	0.009
	6	0.7	0.018	0.53	0.014	0.44	0.01
		Av.	0.019	<b>Av.</b>	<b>0.015</b>	Av.	0.013
		<b>n<sub>c</sub></b>	25.9	<b>n<sub>c</sub></b>	<b>14.34</b>	<b>n<sub>c</sub></b>	11.47

### S6.2D Gradient with different $t_G/t_0$

**Table S2:** Gradient program used for analysis under different  $t_G/t_0$  using the 2.1 mm ID x 50 mm 1.7  $\mu$ m Waters Acquity HSS C18 column, reported in Figure 4.

$t_G/t_0$ %B	2 t (min)	3	4	6	8	10	20	40	100
35	0.00	0.00	0.00	0.00	0.00	0.00	0.00	0.00	0.00
75	0.02	0.03	0.04	0.06	0.08	0.10	0.20	0.40	1.00
100	0.26	0.38	0.51	0.77	1.02	1.28	2.55	5.11	12.77
100	0.30	0.45	0.60	0.90	1.20	1.50	3.00	6.00	15.00